J. Opt. Fiber. Commun. Rep. 2, 435–461 (2005)
© 2005 Springer Science + Business Media Inc.
DOI: 10.1007/s10297-005-0058-9
Editors: Siddharth Ramachandran

JOURNAL OF
Optical and Fiber
Communications Reports

Control of dispersion in photonic crystal fibers

P.J. Roberts[1,2], B.J. Mangan[1], H. Sabert[1], F. Couny[1,2], T.A. Birks[2], J.C. Knight[2] and P.St.J. Russell[2]

[1] Blaze Photonics, University of Bath Campus
Claverton Down, Bath BA2 7AY, UK
[2] University of Bath, Claverton Down, Bath BA2 7AY, UK

Abstract. Photonic crystal fibers (PCFs) exploit the large index difference between air and glass to achieve modal properties unattainable by conventional fiber techniques.

1. Introduction

The photonic crystal fibers (PCF) geometry comprises an array of parallel air holes, generally in a triangular lattice arrangement, running down the length of the fiber. The fibers fall into two distinct classes: those with a solid core which guide by a modified form of total internal reflection, and those with an air core which guide by means of a photonic band gap of the holey cladding. The guidance mechanism of the first type of PCF, an example of which is shown in Fig. 1(a), is analogous to the guidance in conventional MCVD fibers, with the index of the holey cladding region being a particular weighted average of the material indices in this region. The band gap PCFs guide by a less familiar mechanism, with the arrangement of air holes in the cladding causing a gap to open in the modal spectrum of the cladding over a range of effective index values. Figure 1(b) shows a typical fabricated hollow core fiber that operates over a 200 nm wavelength range centered at 1550 nm.

The two classes of PCF have very different mode dispersion, loss and nonlinearity properties. Both classes can nevertheless be used as the basis of dispersion compensating fiber (DCF). The solid core variety has been more extensively explored and developed in a DCF context, and most of the discussion of the current paper will concentrate on this geometry. The emergent technology of hollow core band gap PCF nevertheless provides the potential for achieving compact high quality DCF, or even

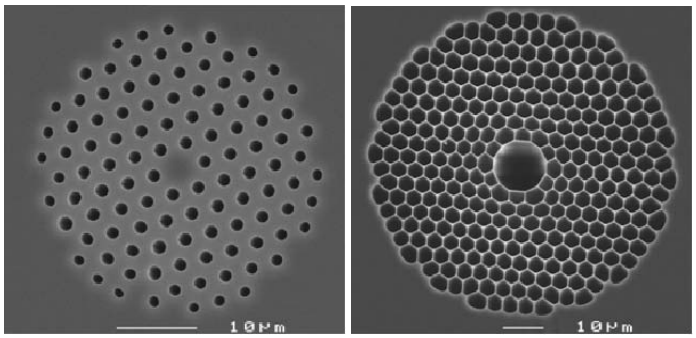

Fig. 1. A SEM of (a) a typical solid core PCF (BlazePhotonics SC-5.0-1040) and (b) a typical hollow core band gap PCF (BlazePhotonics HC-1550-02).

for eliminating the need for dispersion compensation altogether if used as transmission fiber. A section will be devoted to a discussion of this type of fiber.

The dispersion of a guided mode in a solid core PCF can be considered as being due (a) to the material dispersion (since most of the light resides in glass), (b) the confining waveguide effect and (c) the dispersion in the effective index of the cladding region. Strong confinement to a small core region can be achieved with use of a cladding with a large air filling fraction. The resulting high waveguide dispersion can act to cancel even the large negative dispersion of silica glass that exists at visible wavelengths. [1,2] By tailoring the hole spacing and air filling fraction in the cladding, the wavelength at which the dispersion passes through zero can be tuned to a required wavelength. This has been exploited to enhance nonlinear phenomena, a particularly striking example of which is supercontinuum generation, whereby the short high intensity pulses are broadened into a spectrum which can extend over more than an octave. [3,4]

For larger cores, the guided mode dispersion is primarily a consequence of the material dispersion and the cladding index dispersion. For small holes in the archetypal PCF geometry, such as the fiber shown in Fig. 1(a), the effective index of the cladding approaches the index of silica as the wavelength is reduced in such a way that the fiber remains single mode guiding at all wavelengths. [5,6] For this to occur, the diameter of the holes must be less than about 0.42 of the hole spacing Λ.

Exploiting different holes sizes within the cladding region enables a spatial variation in the effective index of the cladding to be realized. [7–12] This opens up the possibility of achieving a highly modified dispersion in the same way as can be achieved by using a modulated index profile in the cladding of conventional MCVD fibers. [13–15] In particular, the "W"-profile and the dual concentric core profile used in conventional MCVD fiber DCFs have PCF analogues in which a radial variation in hole size is imposed. The mechanism of achieving large dispersion by exploiting an anti-crossing of the fundamental mode and a second ring-like mode can be applied to both fiber forms.

High bit rate communication places stringent constraints on the polarization mode dispersion (PMD) and multi-path interference (MPI) that can be tolerated from a dispersion compensating module. Conventional fiber development has taken great steps

to minimize these effects. Particularly notable is the advances is achieving a regular and even doping concentration with a close to circular core and the spinning of the fiber during its draw so as to further reduce the PMD. To compete with MCVD fibers in a communications context, PCF fabrication must of course address these same issues. The microstructure within a PCF imposes new problems for the fiber draw due to the natural tendency of the holes to collapse under surface tension. The holes are prevented from collapsing by applying gas pressure during the draw, but it possible for small fluctuations to grow due to an inherent instability in the process.

To be compatible with current transmission fiber, low loss interfaces must exist between PCF and MCVD fiber forms. The constraint that multi path interference (MPI) imposes on these interfaces in a high bit rate communication system is particularly stringent. Recent advances in adiabatic transforms between standard fiber and PCF, using for example a ferrule, suggests that this might become achievable even for connection to small core PCF forms.

Although PCFs have been around for less than ten years, it is worthwhile at this time to assess their potential for deployment as DCF and compare their properties with current DCF technology. The paper is organized as follows: Section 2 describes how dispersion in PCFs can be modeled and introduces the effective index model for solid core PCFs. Section 3 gives details of the design space available for achieving a negative dispersion characteristic slope-matched to commercial transmission fiber using concentric cores. Section 4 gives an overview of other solid core PCF geometries that could be used for dispersion compensation. Section 5 presents experimental results for a fabricated PCF that shows more (negative) than -1000ps/nm/km dispersion at 1550 nm and is dispersion slope-matched to SMF-28 with a low dispersion curvature. Section 6 discusses the constraints that PMD and MPI impose on the incorporation of a PCF-based compensator in a communication system. Section 7 discusses the prospects for using band gap fibers for dispersion compensation and also considers the implications for dispersion management of using hollow core fiber as transmission fiber. Section 8 draws some conclusions and considers future directions for PCF-based dispersion compensation.

2. Modeling Dispersion in PCFs

2.1. Analogies with Step Index Fibers—The Effective Index Model

Solid core PCFs guide by a modified form of total internal reflection and can often be modeled sufficiently accurately by use of an effective index model. Considering first the archetypal PCF geometry exemplified by the fiber in Fig. 1(a), a single effective index for the cladding region is required for such a model, as well as a size to ascribe to the silica core region. From fitting to the results of rigorous calculations, it has been found [16,17] that taking the effective index of the cladding to be its cut-off index n_{cut} and considering the core to be a circular region of diameter 1.24Λ provides a remarkably accurate description of the modal properties of these solid core PCFs. Here Λ is the distance between the centers of nearest neighbor holes.

The cladding cut-off index n_{cut} can be calculated by a number of different approaches. An accurate yet quick numerical method is to calculate the index of the fundamental space filling mode of the cladding using a band structure code such as

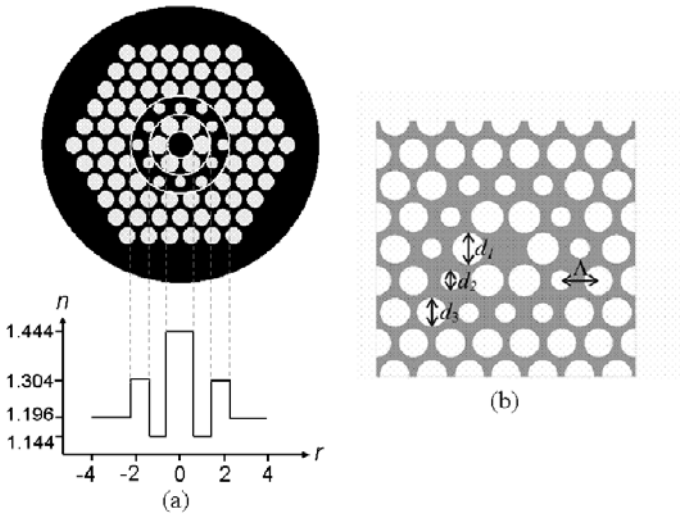

Fig. 2. (a) A solid core PCF design for dispersion compensation, together with its effective index representation that is of a dual concentric core form. The example shown has a pitch $\Lambda = 1.0\mu$m and hole diameters d_1=0.926Λ, $d_2 = 0.619\Lambda$, $d_3 = 0.804\Lambda$ as defined in Fig. 2(b). The effective index variation in the cladding of such a small core and high air filling fraction fiber is many times larger than could be achieved by MCVD technology.

a plane wave approach. The fundamental space filling mode is the mode of highest effective index at the Γ-point of the crystal cladding Brillouin Zone and its index coincides with the cladding cut-off index $n_{\rm cut}$.

Solid core PCFs with a radially modulated hole size, such as the design shown in Fig. 2, can also be modeled approximately using an effective index model. The cladding is divided up into annular regions as shown schematically in Fig. 2, with the area of the jth ring from the center being given by $3\sqrt{3}j\Lambda^2$. The effective index of the jth ring containing holes of diameter d_j can be taken to be the index of the fundamental space filling mode for a triangular lattice arrangement of holes with pitch Λ and hole diameter d_j.

Despite the apparent crudity of the effective index model for the geometry of Fig. 2, it provides a reasonable estimate of the hole sizes and pitch required to achieve a particular dispersion characteristic with minimal computational effort. It also provides an important conceptual framework since it maps the problem onto a form familiar to designers of conventional MCVD fiber DCFs.

To obtain more precise design parameters for solid core fibers, or to adequately model band gap fibers, more accurate analysis is required, a few schemes for which are cited below.

2.2. Rigorous Numerical Approaches

A variety of numerical schemes are available for modeling the dispersion properties of PCFs, most of which have come across from electronic band structure calculations.

The most extensively used approach is based on a plane wave expansion of both the dielectric distribution and the electromagnetic fields within the fiber. The core and a sufficient region of the cladding are included within the supercell over which the Fourier expansions take place. Plane wave schemes operate by finding modes either at a fixed frequency ω, [18] or alternatively at a fixed longitudinal wavevector component β. [19] The fixed ω methods are more suitable since they allow material dispersion to be naturally included, but are slightly more complex to code.

Other numerical approaches that are appropriate for the PCF geometry include a localized basis expansion technique, [20] the finite difference time domain method, [21] finite element [22] and boundary element [23] schemes, and the multipole method. [24] The multipole approach is only appropriate to arrangements of circular holes, but is particularly efficient for mode calculations unless a very large number of holes are required to confine the light. This method is employed in the next section to explore the DCF design space.

3. Solid Core PCF Dispersion Compensators with Concentric Cores

3.1. An Example Small Core PCF Dispersion Compensator

For dispersion compensation of standard commercial fiber such as Corning SMF-28, a negative dispersion D and negative dispersion slope $dD/d\lambda$ are required. The relative dispersion slope RDS $= (dD/d\lambda)/D$ should match as closely as possible that of the fiber being compensated (RDS = 0.0036 nm^{-1} for SMF-28) if multiple wavelength compensation is needed. Since the dispersion curvature of standard transmission fiber is small over the communication bands, this quality should also be reflected in the dispersion compensating fiber if broadband and high bit-rate signal transfer is envisaged.

To achieve the required dispersion properties, a mode anti-crossing event between the fundamental LP_{01}-like mode of the PCF and a mode associated with a ring of relatively small holes (the second ring of the fiber in Fig. 2) can be exploited. Anti-crossing in the wavelength (λ) – effective mode index (n) plane can occur whenever the trajectories of two modes of a waveguide come close together. If interaction between the modes is not forbidden due to a symmetry incompatibility, the modes interact such that the two mode branches of the waveguide repel each other and an anti-crossing is formed. Close to the anti-crossing point, the curvature of the trajectories is large which implies a high dispersion value.

Figure 3(a) shows as an example of a mode anti-crossing for a small core and large air filling fraction DCF, with a pitch Λ of just 1.0 μm, circular holes of diameter d_1 = 0.926Λ in the first ring, d_2 = 0.619Λ in the second ring, the remaining holes having diameter d_3 = 0.804Λ. The fiber is the example shown schematically in Fig. 2 with its effective index representation. The high curvature in the mode indices around the anti-crossing signifies a high dispersion, with the upper branch giving the negative dispersion characteristic shown in Fig. 3(b). The RDS of the upper branch is 0.0038 nm^{-1}, which is close to matching the value for SMF-28.

Figure 4(a) shows the mode field intensity profile of the upper branch at a wavelength of 1.55 μm. Near the center of the core the profile is close to Gaussian, but the intensity levels out somewhat at the ring of smaller holes. Figure 4(b) shows the azimuthally averaged intensity profile as a function of the distance r from the center

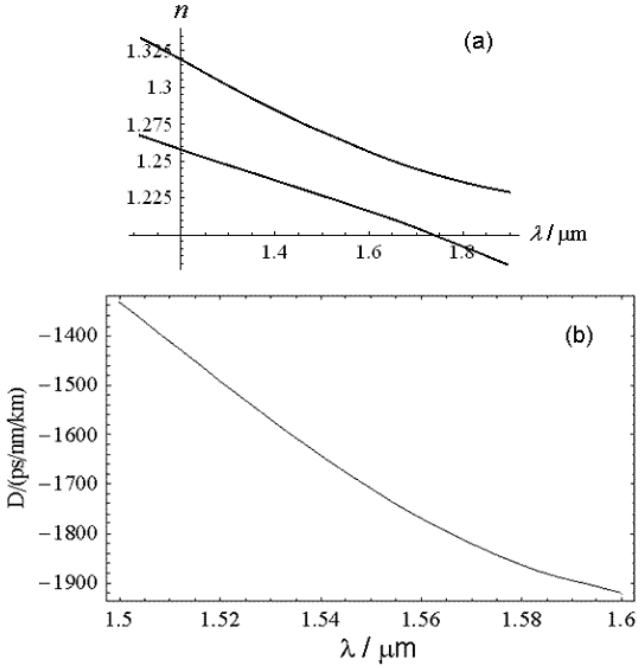

Fig. 3. The mode indices of the LP_{01}-like and ring-like modes are plotted as a function of wavelength λ in (a) for the small core PCF dispersion compensator shown schematically in Fig. 2. The mode interaction causes an avoided crossing with an associated high curvature. The resulting dispersion of the upper (LP_{01}-like over the plotted wavelength range) branch is shown in (b).

of the core, for wavelengths λ = 1.5, 1.55 and 1.6 μm. Within the C-band the field of the mode in the upper branch is not excessively distorted by hybridization with the competing mode associated with the annular ring of smaller holes; the field intensity in this ring is at least 18 dB below the intensity at the mode center and the shape overlap with a conventional LP_{01} fiber mode is above 90%.

Despite mode dispersion being directly linked to a wavelength dependence of the mode shape, Fig. 4(b) shows that the high dispersion of the example DCF appears not to be accompanied by a large wavelength dependence of the field distribution. This is because of the large index difference between silica and air: a small shift of the field from air to silica produces a sizeable change in the mode index.

3.2. The Mode Area vs. Dispersion Trade-Off

In achieving a negative dispersion with a particular relative dispersion slope (RDS), there remains some design freedom. In particular, the effective mode area of the device can be varied over a wide range whilst maintaining suitable dispersion characteristics. The most important driver for the mode area is the nearest neighbor hole spacing Λ,

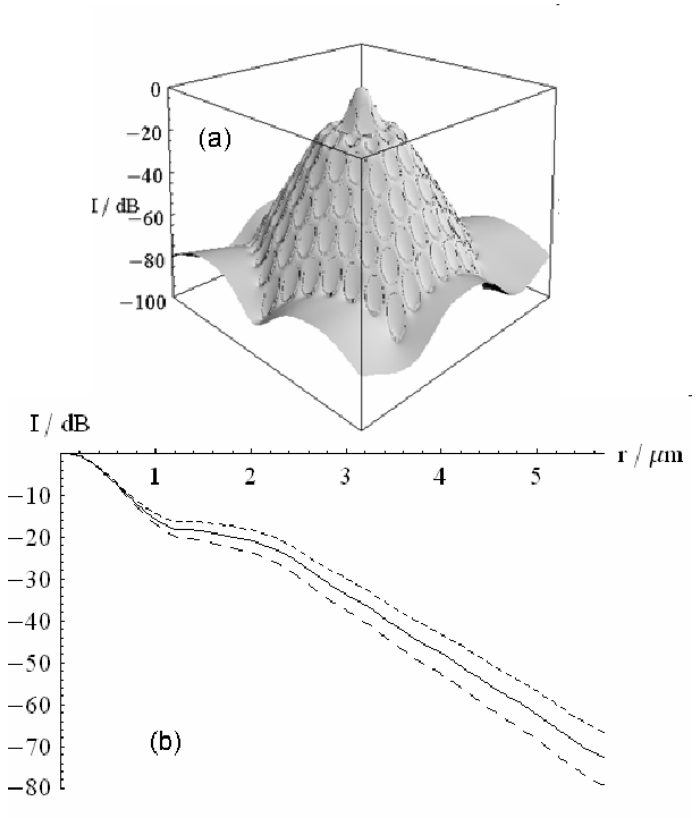

Fig. 4. The mode field intensity distribution at λ = 1.55 μm for the DCF depicted in Fig. 2 is shown in (a). The azimuthally averaged mode intensity distribution is shown in (b) as a function of the distance r from the center of the core at wavelengths λ = 1.5 μm (long dashed curve), λ = 1.55 μm (continuous curve) and λ = 1.6 μm (short dashed curve).

with the mode area expected to increase with Λ. Sets of hole sizes can be found at a chosen hole spacing which give the wanted dispersion characteristic. The discussion will henceforth be restricted to designs with the type of geometry depicted in figure 2, which is determined by three hole sizes d_1, d_2 and d_3, as well as the pitch Λ.

An automatic optimization scheme was adopted to find the highest negative dispersion obtainable for the chosen geometry at the central operation wavelength λ_c = 1.55 μm, as a function of an imposed Λ. Constraints are enforced to ensure the RDS at λ_c is equal to that of a target transmission fiber, such SMF-28, to within a tolerance and also to ensure the dispersion curvature is not too high. A standard simplex algorithm was employed for the optimization, which did not allow for rigid constraints to be imposed. Instead soft constraints were in-built into the cost function $Z\left(d_1, d_2, d_3\right)$ that was minimized. The chosen functional form of $Z\left(d_1, d_2, d_3\right)$ was

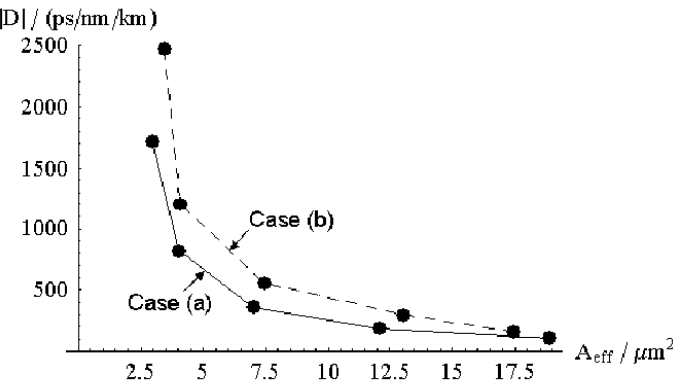

Fig. 5. The dispersion obtained for the DCF designs which are slope-matched to SMF-28, plotted as a function of the mode effective area for the two optimization schemes.

$$Z\left(d_1, d_2, d_3\right) = D + |D| \left\{ a \exp\left[\mu \left| \frac{1}{D} \frac{dD}{d\lambda} - \mathrm{RDS}_t \right| \right] + b \exp\left[\nu \left| \frac{1}{D} \frac{d^2 D}{d\lambda^2} \right| \right] \right\}, \tag{1}$$

where the dispersion D, the RDS $(= D^{-1} dD/d\lambda)$ and the relative dispersion curvature $(D^{-1} d^2 D/d\lambda^2)$ are evaluated at λ_c, and a, b, μ and v are positive-valued parameters which determine the "softness" of the constraints. RDS_t is the relative dispersion slope of the transmission fiber to be compensated.

Figure 5 shows the dispersion value obtained by this procedure plotted as a function of the effective mode area A_{eff}, for a target RDS of $\mathrm{RDS}_t = 0.0036\ \mathrm{nm}^{-1}$ appropriate to SMF-28, and two choices of the parameters a, b, μ and v. The case (a) is for $a = 0.02$, $b = 0.02$, $\mu = 4.0\ \mu$m and $\nu = 0.05\ \mu\mathrm{m}^2$ and case (b) is for $a = 0.02$, $b = 0.02$, $\mu = 4.0\ \mu$m and$\nu = 0.025\ \mu\mathrm{m}^2$. The two cases differ only in the stringency on the dispersion curvature: choice (a) maintains a straighter dispersion characteristic that can match better the dispersion shape of SMF-28 over a wide wavelength band. The straightness of the dispersion curve also affects the sensitivity to the geometrical parameters of the fiber, with a higher curvature indicating a higher sensitivity. Hence maintaining a straighter dispersion characteristic yields a design that is more tolerant to fabrication uncertainties. Both case (a) and case (b) yield designs with RDS values within 10% if the target value RDS_t.

From Fig. 5 it is apparent that the dispersion of the optimized designs decreases with increasing mode area. An important figure of merit (FOM) that assesses the nonlinearity of the DCF can be defined by

$$\eta_{\mathrm{NL}} = A_{\mathrm{eff}}\ |D|\,, \tag{2}$$

a larger value of η_{NL} indicating that higher power can be handled before nonlinear effects become prohibitive. Figure 6a shows the nonlinear figure of merit as a function of mode area A_{eff} for case (a) above, from which it is apparent that the dependence is weak, with η_{NL} decreasing by just a factor of two as the effective mode area is

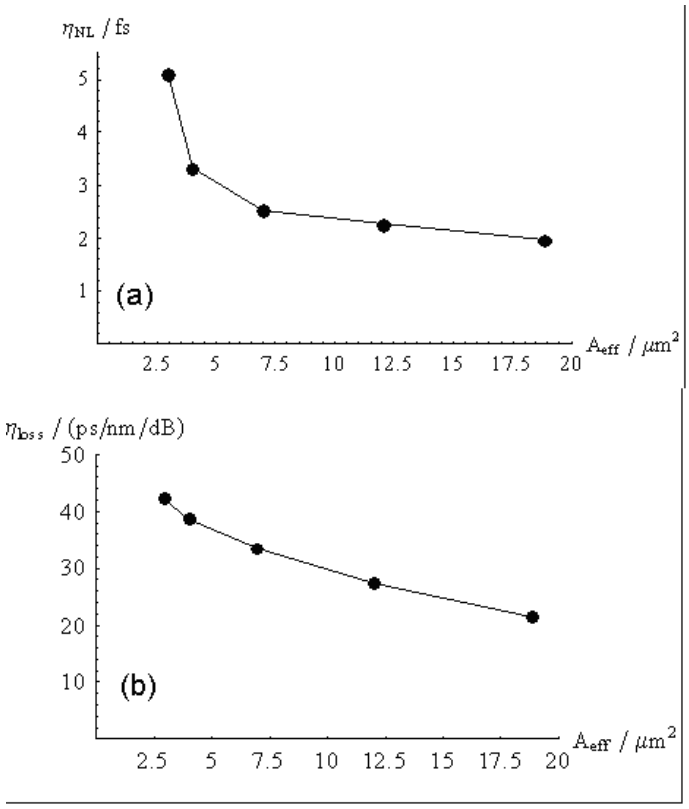

Fig. 6. The (a) nonlinear and (b) loss figure of merits for case (a) DCF designs. The nonlinear figure of merit is comparable to that of a commercial high quality dual concentric core DCF, but the loss figure of merit is inferior by a factor of around ten.

increased from 3 to 20 μm. Hence from a power tolerance standpoint, a small core fiber having an effective mode area of 3 μm^2 actually performs slightly better than a fiber with a mode area of 20μm^2. The smaller mode area is more than balanced by an increase in dispersion that reduces the length of DCF required to compensate a given length of transmission fiber. The nonlinear FOM for a high quality commercially available DCF is around 3.5 fs, which is very similar to the value for the PCF-based compensator.

A second important figure of merit relates to the loss of the compensating fibers. Loss in PCFs is due to bulk Rayleigh scattering and absorption of the glass material (just as in standard fiber), roughness at the hole interfaces and impurity scattering and absorption both at the hole interfaces and within the glass. The roughness scattering loss increases in strength as the normalised field intensity at the interfaces increases. The relative strength of interface scattering can be assessed using the parameter F [25,26] defined by

$$F = \left(\frac{\varepsilon_0}{\mu_0}\right)^{1/2} \frac{\oint_{\text{hole perimeters}} ds\, |\mathbf{E}|^2}{\int_{\text{x-section}} dS\ (\mathbf{E} \wedge \mathbf{H}^*) \cdot \hat{\mathbf{z}}}, \tag{3}$$

where **E** and **H** are the electric and magnetic fields being guided by the fiber. The fields in the numerator integrand are evaluated on the air side of the interfaces. Rayleigh scattering loss at the interfaces can be shown to be accurately governed by the factor F. Even for longer-scale forms of surface roughness, the factor F is found to qualitatively provide a relative measure of the scattering loss that can be expected. [26] In typical fabricated PCFs, the interface roughness scattering loss around a wavelength of 1.55 μm can be estimated using

$$\gamma_{\text{rough}} \Big/ \text{dB km}^{-1} \approx 20\, F \Big/ \mu\text{m}^{-1}. \tag{4}$$

Interface roughness scattering dominates over bulk Rayleigh scattering at this wavelength when F is greater than about 0.01 μm^{-1}.

A loss figure of merit for the DCF can be defined by

$$\eta_{\text{loss}} = D/\text{loss}. \tag{5}$$

This figure of merit increases as the loss of the DCF required for compensating a fixed length of transmission fiber decreases. Figure 6(b) shows η_{loss} for the PCF dispersion compensator, designed according to case (a) defined above, where the loss was assumed to be dominated by interface roughness scattering and to be determined by Eq. (4). The loss FOM for a high quality MCVD DCF is around 450 ps/nm/dB, [27] a factor of about ten higher than for the PCF compensator. It is clear that at current hole interface roughness levels, the incurred scattering loss provides a severe limitation to the loss FOM of solid core PCF-based DCFs of the current design.

The hole size to pitch ratios d_1/Λ, d_2/Λ and d_3/Λ which were found by the optimization procedure for case (a) are shown in Fig. 7 as a function of the imposed pitch Λ. The ratios all monotonically decrease with increasing Λ, the diameter d_3 of the holes which define the outer cladding region approaching 0.31Λ at Λ = 2.0μm. The decrease in these ratios explains why the effective area increases more rapidly than with the square of Λ. All the designs require several rings of the outer cladding material to sufficiently confine the light. The total number of rings of holes required to achieve lower than 1 dB/km leakage loss over the C-band increases from 9 for the Λ = 1.0μm design to 13 for the Λ = 2.0μm design.

The designs with smaller mode area do support modes other than the "fundamental" modes associated with the central core and the high index ring. These modes can, however, be rendered lossy by choosing the number of cladding rings to be just sufficient to guide the fundamental central core mode with adequately low leakage loss over the operational bandwidth. In this way the impact of the higher order modes on multi path interference (MPI) is minimized.

The separation in mode effective index between the two anti-crossing mode braches for the Λ = 1μm design is maintained at a value of at least 0.03, as can be inferred from Fig. 3. This separation does decrease as the mode size increases, but even for the design with mode area close to 20 μm^2, the mode interaction is strong enough for it to remain at a value above 0.0025 over the C-band. This in conjunction with the relatively small mode areas of the fibers implies that macro- and micro- bend induced coupling between the modes small for the devices unless extremely tight bends are attempted.

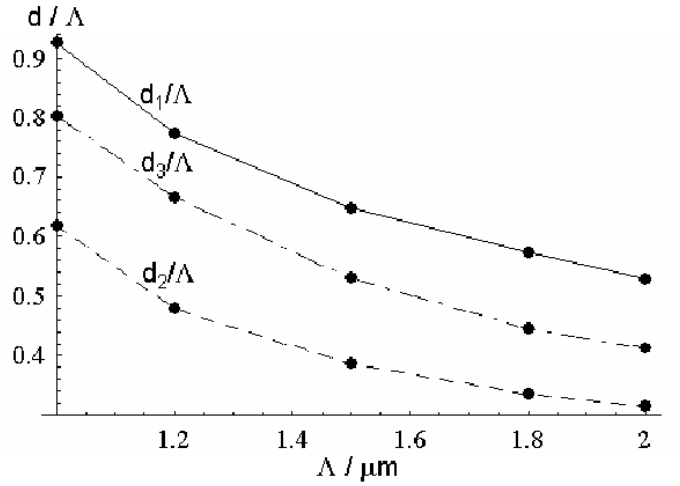

Fig. 7. The normalized hole diameters plotted as a function of the imposed pitch Λ for the SMF-28 DCFs designed according to case (a).

Over the explored mode area range, the amount of the ring-like mode that is admixed to the LP_{01}-like core mode within the C-band is broadly similar for all the designs found with same set of optimization parameters. Likewise the wavelength dependence of the field intensity is similar over the C-band for each design, although the larger pitch designs have less modal power residing within the air holes. These properties are exemplified in Fig. 4 for the 1-μm pitch design.

3.3. Sensitivity to Geometrical Perturbations

To be manufacturable, it is essential that the compensator designs do not show undue sensitivity to the fiber parameters. Current fabrication tolerances with regard to hole spacing and hole sizes lie in the region of 1% at feature sizes appropriate to the compensator designs. The impact this has on the dispersion characteristic will determine the yield that can be expected. The precise value of the dispersion figure attained for a fabricated DCF is not important, as long as it is large and negative, since the fiber can be cut to the length required to compensate the transmission fiber at the central operating wavelength. The RDS and curvature sensitivities then dictate the yield for achieving acceptable values for these parameters.

Figure 8 shows the change of dispersion and RDS produced by 1% changes in the pitch and hole sizes for three designs from case (a) in section 3.2. The geometric changes are amplified by a factor of order 10; this is not surprising, since the high sensitivity to wavelength implied by large dispersion is closely associated with high sensitivity to all other parameters.

The sensitivity is indeed found to increase for designs that possess higher dispersion and dispersion curvature. For example, sensitivities for case (b) of section 3.2 are

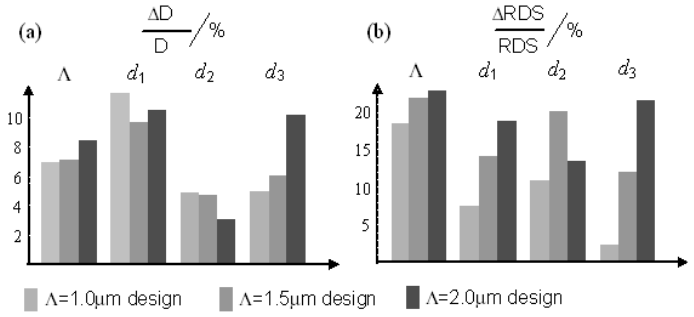

Fig. 8. Sensitivities of (a) the dispersion and (b) RDS of case (a) DCF designs to changes in the fiber parameters. The magnitude of the relative change in these quantities is shown for 1% changes in each of the parameters Λ, d_1, d_2 and d_3.

found to be about twice those for case (a), so that attempting to fabricate a design of higher dispersion figure of merit will adversely affect the yield.

3.4. Compensating Fibers with Large Relative Dispersion Slope

Achieving multi-wavelength dispersion compensation of high RDS transmission fibers, such as large-effective-area-fiber (LEAF) that has an RDS figure of about 0.02 nm^{-1} at a wavelength of 1.55 μm, is more difficult than for standard SMF-28. At a large negative dispersion, the very high dispersion slope needed for a DCF that compensates high RDS fibers is more difficult to maintain over a sizeable wavelength range such as the C-band and the sensitivity to fiber parameters is increased.

A design at $\Lambda = 1.5\mu$m which shows the correct dispersion properties for LEAF compensation is shown in Fig. 9. The structure has hole sizes $d_1 = 0.821\Lambda$, $d_2 = 0.452\Lambda$, $d_3 = 0.590\Lambda$ and was obtained using the case (a) minimization procedure of section 3.2. The dispersion value at a wavelength of 1550 nm is around -1420ps/nm/km, which is somewhat higher than the design in section 3.2 for the SMF-28 compensator at the same mode area ($A_{\text{eff}} = 4.5\ \mu\text{m}^2$). Although the curvature is low at 1550 nm, it rapidly increases beyond the C-band, and the dispersion slope actually becomes positive above a wavelength of about 1580 nm. The sensitivity of the dispersion characteristic to hole sizes and pitch is increased by around a factor of 3 compared to the SMF-28 compensator designs, which is a consequence of the LP_{01}-like mode and the companion ring-like mode coming closer together in effective index in order to achieve the required dispersion characteristic.

Figure 10(a) shows the field intensity distribution for the LEAF compensator at a wavelength of 1550 nm. A comparison with Fig. 4(a) shows that the amount of the outer ring-like mode that admixes with the central core mode is increased for the LEAF compensator, so that the mode is more distorted from a conventional LP_{01} shape than its SMF-28 compensating counterpart. Figure 10(b) shows the azimuthally averaged intensity distribution at wavelengths λ = 1500, 1550 and 1600 nm for the LEAF compensator design. The wavelength dependence of the mode shape is much increased compared to the SMF-28 compensator, c.f., Fig. 4(b).

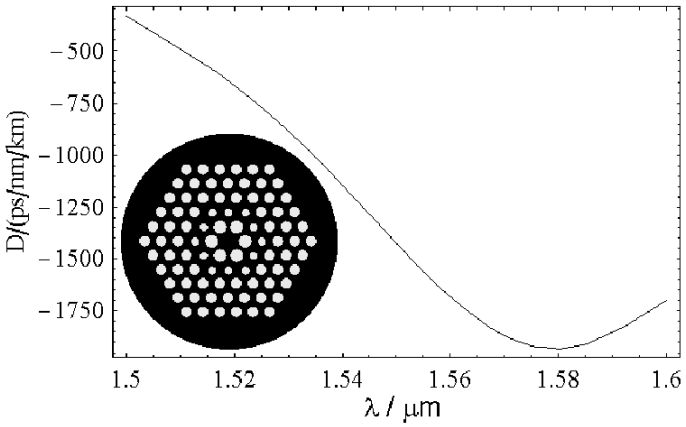

Fig. 9. The dispersion of a LEAF compensating DCF. The fiber, shown schematically in the insert, has pitch $\Lambda = 1.5$ μm and hole sizes $d_1 = 0.821\Lambda$, $d_2 = 0.452\Lambda$ and $d_3 = 0.590\Lambda$. Large negative dispersion is achieved throughout the C-band (1532–1568 nm), but sensitivity to fiber parameters is high. The dispersion curvature and RDS are compromised towards the upper C-band edge.

The two mode branches for the LEAF compensating fiber come closer together within the communication band than they do for the SMF-28 compensating fiber of the same mode area. The separation in index for the fiber of Fig. 9 is nevertheless always at least 0.002 over the C-band, corresponding to a beat-length of less than 1mm. This should be small enough to ensure micro- and macro- bend coupling between the modes is minimal.

4. Other Solid Core PCF Dispersion Compensator Designs

4.1. Small Core PCFs

The design strategy developed above exploits an anti-crossing between the central core mode and a subsidiary ring-like mode. Other designs do exist for achieving high negative dispersion values. The simplest is to use a very small core in a conventional PCF geometry. [1] Such fibers show a dispersion dependence on wavelength that rises to pass through zero, attains a maximum value, and then decreases to pass through zero again. For very small cores, the second zero-GVD crossing wavelength can be significantly smaller than the C-band range and a large negative dispersion with negative slope can be attained around 1550 nm. The problem with this design is its very high loss which is associated with roughness scattering at the hole interfaces, the difficulty of fabricating fibers with sub-micron hole sizes and spacing and in interfacing to standard fiber.

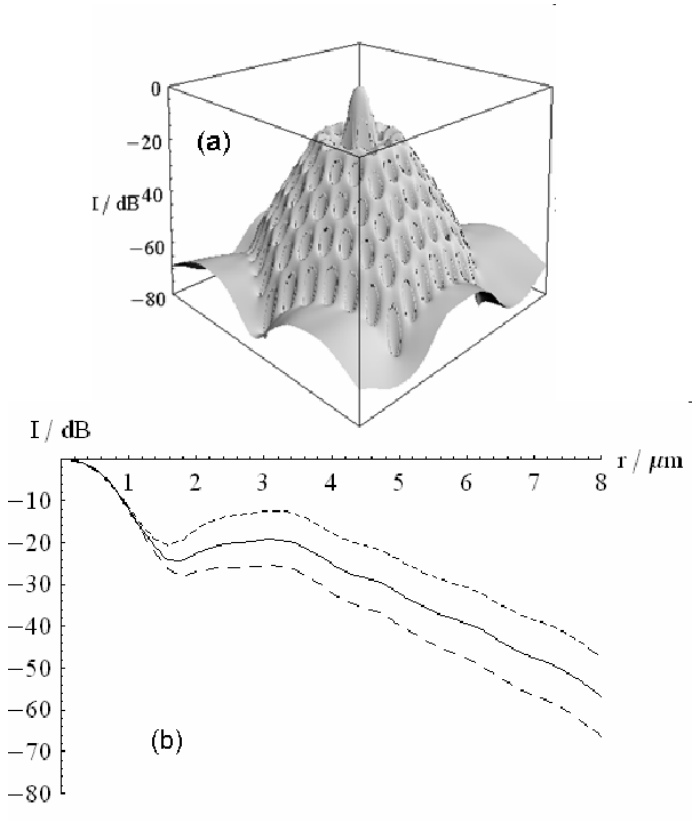

Fig. 10. The mode field intensity distribution at λ = 1.55 μm for LEAF compensating fiber is shown in (a). The azimuthally averaged mode intensity distribution is shown in (b) as a function of the distance r from the center of the core at wavelengths λ = 1.5 μm (long dashed curve), λ = 1.55 μm (continuous curve) and λ = 1.6μm (short dashed curve). The hump at the position of the outer core and the wavelength dependence of the profile is much increased compared to the SMF-28 compensator..

4.2. Operation Near Cut-Off

A mode that is operated close to its cut-off wavelength necessarily shows high dispersion since the degree of confinement is a sensitive function of wavelength. A PCF design in which the holes surrounding the solid core are larger than the outer holes can show such a cut-off in the fundamental (LP_{01}-like) mode, but achieving the correct RDS is not straightforward. Higher order modes (HOMs), which naturally tend to show higher dispersion than the fundamental (LP_{01}-like) mode, can be used as a basis for dispersion compensation. This has been demonstrated with conventional MCVD fibers, [28-30] and the dispersion can be enhanced by operation close to cut-off. The dual concentric core configuration is also appropriate for achieving a large negative dispersion of a chosen HOM with a suitable dispersion slope. A challenge for these

HOM-based compensators is to achieve high efficiency mode transitions between the fundamental mode of transmission fiber and the HOM of the DCF, without incurring unacceptable levels of MPI.

4.3. Other Dual Concentric Core PCF Compensator Designs

A different form of dual concentric core PCF compensator has been proposed [10] which incorporates just two hole sizes. The geometry is the archetypal PCF geometry, comprising a triangular arrangement of air holes surrounding a solid silica core, but the holes around a single ring centered at the solid core are smaller than the others so as to define the outer core region. The authors suggest that incorporation of three airhole layers between the inner and outer cores is optimal for achieving high negative dispersion with acceptable tolerance to structural parameter variations. A dispersion figure of -2200 ps/nm/km was calculated for their structure, but no slope matching to transmission fiber was attempted.

Another dual-core PCF dispersion compensator has been considered in [11]. The geometry comprises the archetypal PCF geometry, but the core is divided into two by incorporation of a ring of 6 much smaller holes. Very large negative dispersions (as high as -18000 ps/nm/km) were calculated for the structure, but over a very narrow wavelength range and with extremely high sensitivity to structural parameter. Fabrication of fibers with very different hole sizes is difficult due to the need to balance surface tension forces

4.4. Doped Core PCF Compensator

A hybrid design, which incorporates a doped core within a graphite crystal arrangement of air holes, has recently been proposed as a means of realizing the dual concentric core geometry. [12] This design has the advantage of requiring just one hole size to be incorporated within the fiber, and dispersions close to those achieved for the 3 hole size geometry in section 3.2 have been predicted at an RDS matched to SMF-28. The mode area at a given dispersion value is comparable to that achieved with the 3 hole size structure, since both geometries are describable by an effective index model with similar effective index profiles. A disadvantage of the doped core design is that high concentrations of Ge (or other index increasing dopant) are required, which can significantly increase the nonlinearity at a given mode effective area. The structure is nevertheless a good candidate for achieving a high loss figure of merit.

5. Fabricated Example of a Dispersion Compensating PCF

Silica photonic crystal fibers are generally fabricated using a stack and draw technique. A set of capillary tubes of equal outer diameter is stacked in a triangular lattice arrangement. A solid silica tube that will become the guiding core is incorporated at the center of the stack. The inner diameter of the tubes in the stack depends on the distance from the central core in a manner that parallels the hole size variation required in the final fiber. The stack, which typically has a cross sectional diameter of around 30 mm, is then drawn down in a furnace to a cane with a diameter of order 2 mm. The

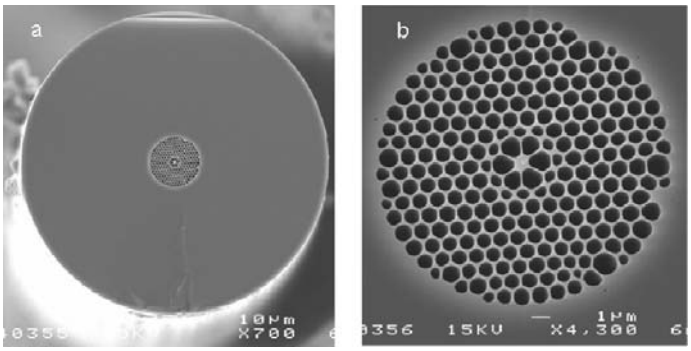

Fig. 11. SEMs taken at two magnifications of a fabricated DCF, which is slope matched to SMF-28. The outer diameter of the fiber is 105 μm and the core is less than a micron across. The structure is intentionally birefringent.

cane is inserted within a capillary jacket tube and the assembly is then drawn to fiber. Water and impurity reduction techniques are employed during the process just as in conventional MCVD fiber production.

As a demonstration of the high dispersion values that can be achieved for a slope-matched DCF using PCF technology, small core fibers have been fabricated based on the design strategy described in section 3.2. [31] Figure 11 shows SEMs of one such fiber with a core diameter of just 1 μm. The holes close to the core are deformed somewhat from being circular, and this does affect the dispersion characteristic of the fiber. The hole deformations can easily be taken into account, using for example a plane wave method, to design a fiber with a particular target RDS. Such studies show that the attainable dispersion at a target relative dispersion slope is not significantly compromised. The sensitivity to small perturbations are also found not to adversely affected by the inner-hole shape deformations.

The fiber shown in Fig. 11 was fabricated to be polarization maintaining: two of the six holes that surround the core are smaller than the other four. Several fibers showing similar dispersion and RDS characteristics were also fabricated without intentional birefringence being imposed. Despite the attempt to fabricate polarization independent fibers, small perturbation are found to persist down the length of a fabricated fiber which result in a differential group delay (DGD) of several ns/km in fibers with such a small core. Since significant birefringence is inevitable, it was decided to enhance the polarization maintaining properties by deliberately increasing the polarization mode splitting, but not to such an extent that the spatial distribution of the fields becomes strongly perturbed. The motivation for exploring PM compensating fibers will be discussed in more detail in section 6.

Figure 12 shows the measured dispersion of the two polarization states associated with the fundamental (LP_{01}-like) spatial mode. The dispersion of one of the polarized states is around -1210 ps/nm/km at a wavelength of 1550 nm and shows a near linear dispersion characteristic over the measured wavelength range with an RDS of 0.004 nm^{-1}, which is within 15% of the figure for SMF-28. The effective mode area of the fiber is calculated to be just 2.0 μm^2, so that the nonlinear FOM is 2.4 fs, a value 1.5

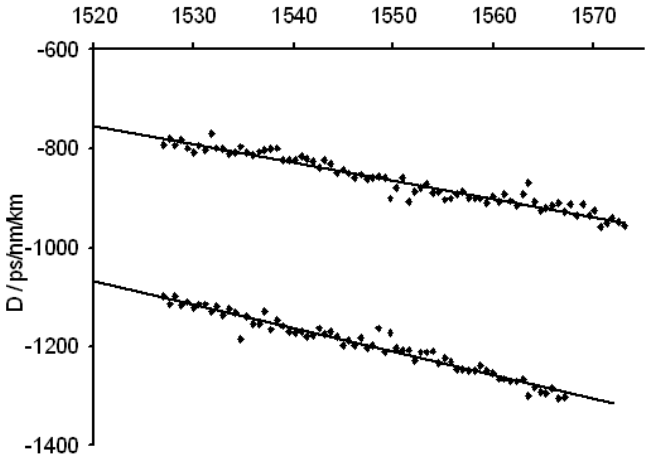

Fig. 12. Measured dispersion of both polarization modes of the fabricated birefringent DCF. The more dispersive mode gives RDS = 0.004 nm^{-1}, which is close to the value for SMF-28. The dispersion of this mode at 1550 nm is −1211 ps/nm/km.

times smaller than for a highest quality commercial DCF. The mode profile, which was calculated directly from a SEM image of the fabricated fiber, is shown in Fig. 13. It is seen that the field penetrates some way into the holey region, with the intensity having decayed only by about 5 dB from its central peak value as it enters the first ring of holes.

Owing to the small size of the core and the high air filling fraction in the cladding of the fabricated fiber, the birefringence level imparted by the relatively small geometrical breaking of six-fold symmetry is substantial. The splitting in effective index of the polarization states is found to be around 0.009 within the C-band, and the differential group delay was measured to be 45 ns/km. The difference in the dispersion levels of the two polarization channels is also sizeable at about 200 ps/nm/km, as can be inferred from Fig. 12.

The loss of the fabricated fiber is high, at around 100 dB/km, which can mostly be attributed to the very high hole interface fields associated with such a small core fiber. The loss FOM is around 25 times lower than for a high performance commercial DCF.

6. PMD and MPI Properties of Solid Core PCF Compensators

6.1. Current PMD Levels of PCF

In a communication system it is generally required to ensure that any inline components operate as far as possible in a polarization independent manner. Arbitrary and time-varying states of polarization pass through the system and pulse spreading or splitting due to PMD or residual birefringence must be maintained at very low levels in high

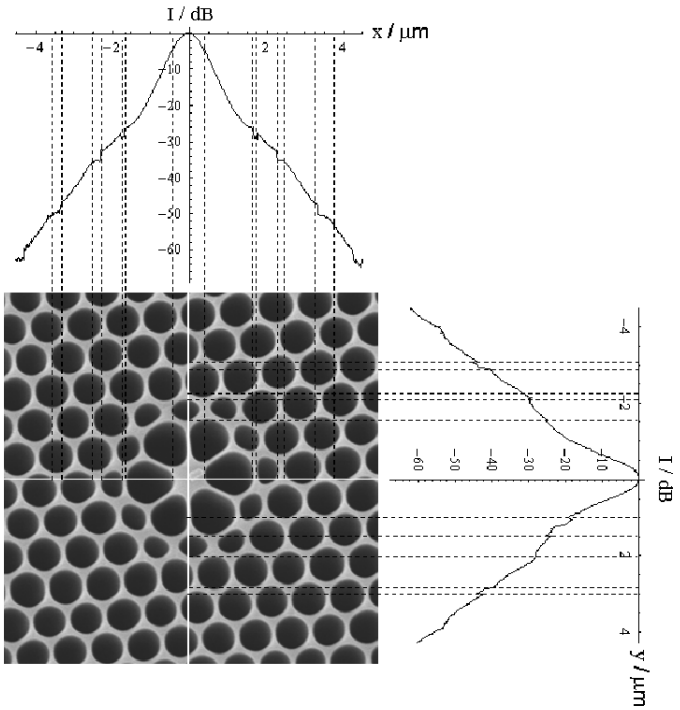

Fig. 13. The mode intensity for one polarization state of the fabricated fiber at a wavelength of 1.55 μm, calculated directly from the SEM image. The intensity profiles are shown along the white horizontal and vertical lines that pass through the center of the fiber core. The intensity has dropped by only 5 dB from its peak value as it enters the fist ring of holes, so hole interface scattering loss is high.

bit rate communication. As an example, the PMD level for 10 GB/s single channel communication over 1000 km must be maintained below about 100 ps over the span length. A span of this length will comprise many components, including around 15 transmission line and amplifier stages and a similar number of dispersion compensating units. If of order 100 separate components are needed, assuming the polarization evolves in a stochastic manner so that PMD over the span increases roughly with the square root of the number of components, one can estimate that a maximum of about a picosecond of PMD can be tolerated for each DCF unit. This is a stringent requirement for PCF-based compensators to achieve. Current commercially available DCF has reached PMD levels as low as 0.5 ps for a unit designed to compensate 80 km of SMF-28, but such low levels are currently far from being achievable with PCF at a mode size compatible with attaining a suitable dispersion characteristic for dispersion compensation.

Unintentional form birefringence in PCFs causes the fibers to show substantial PMD. A Monte-Carlo simulation has been performed in which the hole sizes suffer

from random variations which are maintained along the length of the fiber. Each hole is assumed statistically independent of the others and its diameter is drawn from a Gaussian distribution centered at the hole diameter for the target non birefringent DCF structure. The differential group delay that is incurred by just 1% fluctuations about the six-fold target structure is around 3 ns/km at an effective area of 3 μm^2 and is about 100 ps/km at an effective area of 20 μm^2. If hole sizes are maintained along the length of fiber, this implies the PMD (or rather the differential group delay) figure for the PCF-based DCF will be at least two orders of magnitude higher than the acceptable level for use in a high bit-rate communication system.

In practice some variation of hole diameter with length will occur which will lessen the birefringence level to some degree. Random coupling between the polarization states leads to a diffusive evolution of the polarization state which is characterized by a length scale L_{corr} for state de-correlation and signaled by a square root dependence of PMD on the fiber length. Fabricated PCFs with mode areas of 20 μm^2 or less tend to have large values of L_{corr} so that the lessening of pulse spreading or splitting due to random polarization coupling is minimal. It appears that the variations of the individual hole sizes along the length of the fiber are correlated so that the direction of the axis of polarization is maintained; the dominant variation is typically just a congruent scaling of the entire cross section. The correlation length could be substantially reduced by spinning the fiber as it is drawn, which would significantly reduce the level of PMD. This technique, familiar in conventional MCVD fiber fabrication, has just begum to be developed for PCF, with initial results showing a twenty-fold decrease in the level of PMD for a large mode area fiber. [32] Achieving PMD reduction for the smaller mode area DCF fibers presents a considerably greater challenge.

6.2. Schemes to Combat PMD and Their Impact on MPI

Since PMD constraints are not met by current non polarization preserving solid core PCF-based dispersion compensating fibers, schemes which involve PM compensators have been explored. Since the DCF is required to deal with arbitrary input polarization, just a single pass through a length of PM fiber will not suffice. One scheme to achieve polarization independent characteristics is to splice a length of PM fiber to the same length of identical fiber that has been rotated so that its fast axis is 90 degrees to the fast axis of the first fiber. This is shown schematically in figure 14a. The challenge for such a scheme is to achieve a high efficiency transfer at the splice between the fast and slow polarization states. The highly stringent limitation on multi-path-interference (MPI) in a communication system [33] appears very difficult to meet: the splice must not give rise to a reflected pulse of power greater than about -30 dB to be acceptable. Beyond the MPI issue, maintaining the cancellation of the differential group delay to the required level over a range of wavelengths such as the C-band, as well as a range of operating temperatures, is also found to be difficult. The demands on the polarization maintenance are also high: the polarization extinction ratio (PER) level needs to be maintained at better than about 30 dB over the length of the DCF.

Alternative schemes in which a circulator or Faraday rotators are used in conjunction with a PM fiber have also been considered and are shown schematically in Figs. 14(b)–(d). The set up in Fig. 14(b) ensures the components of an arbitrary incident polarization state propagate in one polarization state of the fiber in one pass through the fiber and in the other fiber polarization state in the other pass. In the schemes shown in

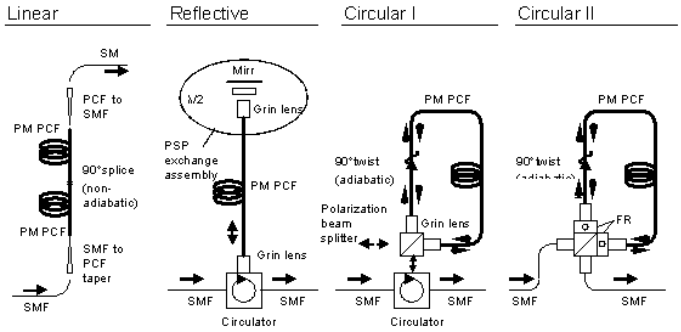

Fig. 14. Candidate schemes to enable the use of a PM compensating fiber in a transmission system.

Figs. 14(c) and 14(d), only one polarization state of the fiber is employed independent of the input polarization. The alternative designs, at the expense of added complexity, act to remove the need for a highly efficient splice and also reduce or eliminate any impact from PMD. Unfortunately, they can be shown to suffer from unacceptable levels of MPI. Even if the efficiency of the polarizing beam splitters is high enough, first order backscattering within the fiber will contribute to the MPI signal. This will be many times higher than the level of second order backscattering which is relevant to a standard DCF setup involving just a single pass through the fiber. For a DCF compensating about 80 km of transmission fiber, one can estimate the level of MPI noise due to first order Rayleigh backscatter to be of order -30 dB relative to the main signal, which is about 30 dB higher than an acceptable figure.

Despite the restrictions imposed by MPI on the use of a PM DCF in a communication system, PM designs are useful to obtain compression or pre-chirp of pulses emitted from a laser source which are subsequently transmitted through a dispersive element such as a fiber. This provided the motivation for developing the fiber described in section 5.

6.3. Other Causes of MPI

Random signal fluctuations induced by MPI can build up over long transmission distances and severely hamper high bit rate communication. For this reason, each constituent of the transmission system should not introduce MPI noise above about -60 dB compared to the main signal intensity. The MPI can be incurred at transitions between different elements in the transmission system, as well as within distributed components such as the transmission fiber itself and dispersion compensating fiber. Although the use of adiabatic mode transformations can at least in principal solve the interfacing problem, scattering events within a fiber provide an intrinsic source of MPI.

For a single pass through a fiber, two scattering events are required to cause the interference in the forward propagating signal mode. Within a single mode transmission fiber such as SMF-28, the dominant MPI contribution comes from double Rayleigh scattering. The first scattering event causes a reflection of a small fraction of the signal

into the backward propagating guided mode and the second reflects a fraction of this power back into the forward propagating mode.

In the DCF, other pathways exist for the creation of MPI within the fiber. Scattering into the ring-like mode, followed by scattering back into the forward propagating LP_{01}-like signal mode, can give a larger contribution to MPI than the double reflection events described above. Although the ring-like mode is lossier than the LP_{01}-like mode, it nevertheless survives typically over several meters so that a large range of temporal delays in the MPI signal can result. Higher order modes of the DCF, which are rendered lossy due to scattering processes and leakage loss, also contribute to the MPI. A detailed exploration of the MPI has not been attempted, but it is estimated that the contribution from the solid core PCF-based DCF in a conventional single pass setup will be similar to that from the transmission fiber it compensates. The estimate is based on considering double scattering events which result in light re-entering the forward propagating signal mode. Fortunately, the capture probability from scattering at the hole interfaces is substantially reduced due to the relatively low normalized intensity of the signal mode at these positions. Since the magnitude of the dispersion of the DCF is many times that of the transmission fiber, the amount of loss due to distributed scattering along the DCF is far smaller than that in the transmission fiber it compensates. These two favorable properties act to cancel the effect of the much enhanced NA associated with the small core DCF (the cross section for double Rayleigh scattering from within the core is roughly proportional to the fourth power of the NA).

As discussed in the previous subsection, the PMD mitigating schemes involving a circulator or Faraday rotator are subject to very high levels of MPI from single scattering events.

7. Prospects for Hollow Core Photonic Crystal Fiber

7.1. Dispersion Compensation Using HCPCF

Whereas solid core PCF compensating fibers behave in a very similar way to conventional MCVD fiber DCFs, the prospect of using band gap fibers opens new possibilities in dispersion management. In contrast to solid core transmission fibers in which material dispersion dominates, the dispersion in hollow core photonic crystal fiber (HCPCF) is due to the waveguide geometry. The dispersion notionally breaks down into two components: that associated with the wavelength dependence of the confining properties of the band gap cladding and that which arises as a natural consequence of confinement. The former component increases as the band gap edges are approached and the field penetrates progressively further into the cladding, whereas the latter component is shown even by a metallic waveguide that allows no penetration of the field into the cladding.

The dispersion of a typical hollow core photonic crystal fiber (HCPCF) is shown in Fig. 15 together with its loss. The shape of the dispersion curve is very characteristic of band gap guidance, with large negative dispersion shown towards the short wavelength side of the band gap and large positive dispersion shown at the high wavelength end: this behavior is a fundamental consequence of a Kramers-Kronig relation operating in the presence of a gap in the density of states. Superimposed on this dispersion is an overall positive shift of around 80 ps/nm/km which may be ascribed to the mode

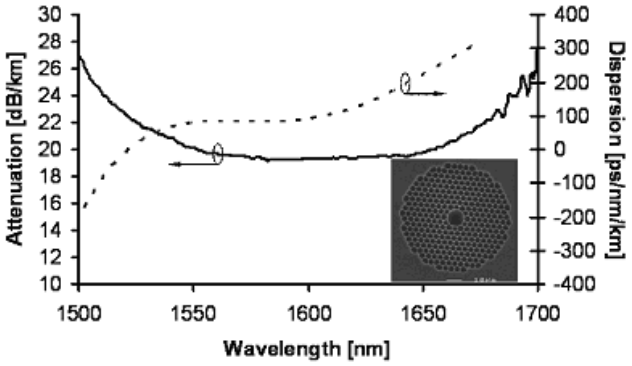

Fig. 15. The dispersion and loss of a typical fabricated HCPCF with a core formed from the omission of seven capillaries (BlazePhotonics fiber HC-1550-02).

confinement effect, although this figure is around three times the dispersion shown by a metallic waveguide with the same core area.

The large negative dispersion close to the short wavelength band gap edge can be used for pre or post-compensation of short pulses from a laser source. [34–37] For the example fiber of Fig. 15, a dispersion of -100 ps/nm/km is associated with just a 25% increase in loss compared to its minimum value of 18 dB/km, whereas a dispersion of -200 ps/nm/km is attained at the expense of a 40% increase in loss. The slope of the dispersion curve is unfortunately positive at such negative dispersion values. To be of use in most communication systems, some degree of RDS matching to the transmission fiber is necessary.

The dispersion properties within the band gap can be altered from the form exemplified in Fig. 15 if an anti anti-crossing occurs between the LP_{01}-like mode and another mode. Such events can occur due to occurrence of modes in the band gap that are associated with the core surround. They are signaled by very rapid and large changes in dispersion and loss. To be able to controllably tune the dispersion and its slope over a sizeable wavelength range such as the C-band and not incur too much of a loss penalty, it is necessary to employ an anti-crossing of the LP_{01} mode with a more air-like mode, perhaps associated with a secondary core situated outside the central air core. The design philosophy then parallels the one used for solid core DCFs.

To incorporate HCPCF for dispersion compensation within a system that uses conventional solid core transmission fiber, low reflection and low loss interfacing solutions will need to be developed. This provides a significant challenge in itself since the mode index of an air guided mode is close to (and just below) unity, whereas the mode index for the solid core fiber is close to the index of silica.

7.2. HCPCF as Transmission Fiber: Is Dispersion Compensation Necessary?

There is a much publicized conjecture that hollow core fibers will reach loss levels below those of conventional fiber and be used directly as transmission fiber. As well as

achieving low loss, it is necessary for the fiber to show sufficiently low levels of PMD and MPI. Whereas the loss levels are rapidly being reduced, with the current reported record standing at 1.7 dB/km, [38] little attention has been paid to PMD and MPI. To achieve the necessary PMD levels, the precision in the manufacturing process will need to be improved and it is likely that the fiber will need to be spun during the fiber draw. MPI also presents a problem, since several long-lived modes other than the one carrying the signal exist within the band gap in current HCPCFs.

If HCPCFs can satisfy the loss, PMD and MPI criteria for use as transmission fiber, there exists the potential for dispensing with dispersion compensating units altogether. This is because the nonlinear coefficient of these fibers can be a thousand times lower than that of a solid fiber, [37] which implies that a much lower dispersion can be tolerated at a fixed power level before nonlinear effects become prohibitive. It remains to design a HCPCF fiber that maintains a low dispersion over an appreciable wavelength window.

8. Conclusions and Future Prospects for PCF-Based Dispersion Compensation

Photonic crystal fibers (PCFs) can be tailored to show a negative dispersion that is slope-matched to transmission fiber such as SMF-28. The large index step between silica and air can be exploited to achieve very large dispersion values whilst maintaining an acceptable tolerance of the dispersion characteristic to the structural parameters of the fiber. The dispersion level achievable at a practical sensitivity level is inextricably linked to the mode area: the smaller the mode area, the larger the dispersion that can be attained. As a consequence, the nonlinearity figure of merit of the fiber for compensating a given length of transmission fiber is only very weakly dependent upon mode area. The loss figure of merit also shows a relatively weak dependence upon mode area, but is currently inferior to this figure for commercial DCFs based on MCVD fiber technology.

Dispersion compensators based on solid core PCFs can be approximately described using an effective index model. This model maps the complex PCF geometry to a radially dependent refractive index profile analogous to the index distributions used in MCVD DCFs. For mode areas greater than about $15\mu m^2$, the index variation inferred from the model is at a level attainable by glass doping technology. This implies that the dispersion characteristics and design constraints of PCF-based DCFs with such mode areas can be expected to be very similar to those of established MCVD DCFs.

In order to compete with MCVD fiber technology in a communication system, DCFs based on solid core PCFs must overcome two main hurdles. The first is loss, which appears to be governed mainly by the roughness at the hole interfaces and the extent to which this can be reduced is at present unclear. A solid-core PCF-based dispersion compensator with a mode area of around 20 μm^2 is expected to show a loss of around 5 dB/km, which is several times higher than the 0.6 dB/km of a commercially available DCF with a similar mode area. The second obstacle to overcome is that of polarization mode dispersion (PMD). This effect becomes more severe as mode area decreases, but even at a mode area of around $20\mu m^2$ is currently at a level that is unacceptable in long haul high bit-rate communication systems. To reduce the figure to an acceptable level will require a substantial increase in the geometrical precision of the fabrication process, and it is likely that the fiber will need to be spun during the

drawing process. Schemes which involve using a polarization maintaining PCF-based DCF can be explored, but to be able to handle an arbitrary input polarization state, they require complicated elements to be introduced which cause unwanted multi-path-interference (MPI) effects.

Although solid-core PCF-based DCFs are currently outperformed by conventional DCFs in a communication system context, they do offer a simple, compact means of achieving pulse compression or pre-chirp in some optical set-ups. Here the high degree of polarization maintenance possible in Hi-Birefringence PCF fibers can be exploited if the polarization direction of the output from a laser is aligned with the polarization axis of the fiber. The highly dispersive fiber forms also find application as highly compact True Time-Delay lines [39] in which pulses centered at slightly different wavelengths become temporally separated.

The use of hollow core photonic crystal fiber (HCPCF) as transmission fiber offers the exciting possibility of eliminating the need for dispersion compensation. Since the nonlinearity of these fibers is much lower than in solid core fibers, operation at low dispersion values can be tolerated. The challenge in the development for HCPCF transmission fibers is to achieve loss figures comparable or better than standard fiber, whilst maintaining an acceptably low level of PMD and MPI. It is also required to design and fabricate a fiber that shows a low dispersion over a significant waveband. None of these goals has yet been demonstrated.

Large negative dispersion can be obtained using HCPCF, making it a candidate for use as DCF. Indeed, this characteristic has been used for compression and pre-compensation of high power laser pulses. To be appropriate for dispersion compensation in a multi-channel communication system, some degree of slope matching to the transmission fiber is necessary. This might be achieved by exploiting an anti-crossing event, just as in solid core DCFs. A detailed exploration of the dispersion compensating possibilities of the hollow core fibers has yet to be carried out.

Acknowledgments

Most of the content of this paper is based on work done by the R&D team of Blaze Photonics. The authors would particularly like to thank L. Farr, D. Williams and M. Mason

References

1. T.A. Birks, D.Mogilevtsev, J.C. Knight and P.St.J. Russell, Dispersion compensation using single-material fibers, IEEE Photon. Technol. Lett., **11**, 674 (1999).
2. J.C. Knight, J. Arriaga, T.A. Birks, A. Ortigosa-Blanch, W.J. Wadsworth, and P.St.J. Russell, Anomalous dispersion in photonic crystal fiber, IEEE Phot. Technol. Lett., **12**, 807 (2000).
3. J.K. Ranka, R.S. Windeler, and A.J. Stentz, Visible continuum generation in air-silica microstructure optical fibers with anomalous dispersion at 800 nm, Opt. Lett., **25**, 25 (2000).
4. S. Coen, A.H.L. Chau, R. Leonhardt, J.D. Harvey, J.C. Knight, W.J. Wadsworth, and P.St.J. Russell, White-light supercontinuum generation with 60-ps pump pulses in a photonic crystal fiber, Opt. Lett., **26**, 1356 (2001).

5. J.C. Knight, T.A. Birks, P.St.J. Russell, and D.M. Atkin, All-silica single-mode optical fiber with photonic crystal cladding, Opt. Lett., **21**, 1547 (1996).
6. T.A. Birks, J.C. Knight, and P.St.J. Russell, Endlessly single-mode photonic crystal fiber, Opt. Lett., **13**, 961 (1997).
7. F. Poli, A. Cucinotta, S. Selleri, and L. Vincetti, Characterisation of microstructured optical fibers for wideband dispersion compensation, J. Opt. Soc. Am. A **20**, 1958 (2003).
8. F. Poli, A. Cucinotta, S. Selleri and A.H. Bouk, Tailoring of flattened dispersion in highly nonlinear photonic crystal fibers, IEEE Photon. Technol. Lett., **16**, 1065 (2004).
9. L.P. Sheng, W.P. Huang, G.X. Chen, and S.S. Jian, Design and optimization of photonic crystal fibers for broad-band dispersion compensation, IEEE Phot. Techn. Lett., **15**, 540 (2003).
10. F. Gerome, J.-L. Auguste and J.-M. Blondy, Design of dispersion-compensating fibers based on dual-concentric-core photonic crystal fiber, Opt. Lett., **29**, 2725 (2004).
11. Y. Ni, L. Zhang, L. An, J. Peng, and C. Fan, Dual-core photonic crystal fiber for dispersion compensation, IEEE Photon. Technol. Lett., **16**, 1516 (2004).
12. B. Zsigri, J. Laegsgaard, and A. Bjarklev, A novel photonic crystal fiber design for dispersion compensation, J. Opt. A: Pure Appl. Opt., **6**, 717 (2004).
13. A.J. Antos and D.K. Smith, Design and characterization of dispersion compensating fiber based on LP_{01} mode, IEEE J. Lightwave Technol., **12**, 1739 (1994).
14. L. Grüner-Nielsen, S.N. Knudsen, T. Veng, B. Edvold, and C.C. Larsen, Design and Manufacture of Dispersion Compensating Fiber for Simultaneous Compensation of Dispersion and Dispersion Slope,' Tech. Dig. OFC'99, Paper WM13, p. 232, 1999.
15. L. Grüner-Nielsen, S.N. Knudsen, P. Kristensen, T. Veng, B. Edvold , and T. Magnussen, Dispersion Compensating Fibers and Perspectives for Future Developments, Proc. Europ. Conf. Opt. Comm. ECOC'2000, Vol. 1, p. 91, 2000.
16. A. Birks, D.Mogilevtsev, J.C. Knight, P.St.J. Russell, J. Broeng, P.J. Roberts, J.A. West, D.C. Allan, and J.C. Fajardo, The analogy between photonic crystal fibers and step index fibers, in Optical Fiber Communication Conference, OSA Technical Digest, Optical Soc. of America, Wash. DC, p. 114, 1999.
17. J.C. Knight, T.A. Birks, P.St.J. Russell and J.P. deSandro, Properties of photonic crystal fiber and the effective index model, J. Opt. Soc. Am. A **15**, 748 (1998).
18. J.M. Pottage, D.M. Bird, T.D. Hedley, T.A. Birks, J.C. Knight, P.St.J. Russell, and P.J. Roberts, Robust photonic band gaps for hollow core guidance in PCF made from high index glass, Opt. Express, **1**, 285 (2003).
19. S.G. Johnson and J.D. Joannopoulos, Block-iterative frequency-domain methods for Maxwell's equations in a planewave basis, Opt. Express, **8**, 173 (2001).
20. D. Mogilevtsev, T.A. Birks, and P.St.J. Russell, Localized function method for modeling defect modes in 2-D photonic crystals, J. Lightwave Technol., **17**, 2078 (1999).
21. R. Ghosh, A. Kumar, J.P. Meunier, and E.. Marin, Modal Characteristics of Few-mode Silica-Based Photonic Crystal Fibers, Opt. Quant. Electron., **32**, 963 (2000).
22. S. Guenneau, A. Nicolet, F. Zolla, and S. Lasquellec, Modeling of photonic crystal optical fibers with finite elements, IEEE Trans. Magn. (USA), **38**, 1261 (2002).
23. N. Guan; S. Habu, S.K. Takenaga, K. Himeno, and A. Wada, Boundary element method for analysis of holey optical fibers J. Lightwave Technol., **21**, 1787 (2003).

24. T.P. White, B.T. Kuhlmey, R.C. McPhedran, D. Maystre, G. Renversez, C.M. de Sterke and L.C. Botten, Multipole method for microstructured optical fibers: 1. Formulation, J. Opt. Soc. Am. B, **19**, 2322 (2002).

25. L. Farr, J.C. Knight, B.J. Mangan, and P.J. Roberts, 'Low loss photonic crystal fiber, European Conference on Optical Communication (ECOC 2002), Copenhagen Denmark, post-deadline paper PD13, 2002.

26. P.J. Roberts, F. Couny, H. Sabert, B.J. Mangan, D.P. Williams, L. Farr, M.W. Mason, A. Tomlinson, T.A. Birks, J.C. Knight, and P.St.J. Russell, Ultimate low loss of hollow-core photonic crystal fibers, Opt. Express, **13**, 236 (2005).

27. M. Wandel, T. Veng, Q. Le, and L. Grüner-Nielsen; Dispersion compensating fiber with a high figure of merit, Proceedings of 2001 European Conference on Optical Communications, Paper PD.A.1.4, 2001.

28. C.D. Poole, J.M. Wiesenfeld, A.R. McCormick, and K.T. Nelson, Broadband dispersion compensation by using high-order spatial mode in a two-mode fiber, Opt. Lett., **17**, 985 (1992).

29. C.D. Poole, J.M. Wiesenfeld, D.J. DiGiovanni, and A.M. Vengsarkar, Optical fiber-based dispersion compensation using higher order modes near cutoff, J.l Lightwave Technol., **12**, 1745 (1994).

30. S. Ramachandran, B. Mikkelsen, L.C. Cowsar, M.F. Yan, G. Raybon, L. Boivin, M. Fishteyn, W.A. Reed, P. Wisk, D. Brownlow, and R.G. Huff, L. Gruner-Nielsen, All-fiber grating-based higher order mode dispersion compensator for broad-band compensation and 1000-km transmission at 40 Gb/s, IEEE Phot. Techn. Lett., **13**, 632 (2001).

31. B.J. Mangan, F. Couny, L. Farr, A. Langford, P.J. Roberts, D.P. Williams, M. Banham, M.W. Mason, D.F. Murphy, E.A.M. Brown, H. Sabert, T.A. Birks, J.C. Knight, and P.St.J. Russell, Slope-matched dispersion-compensating photonic crystal fiber, Technical Digest Conference on Lasers and Electro-Optics, CLEO'04, San Francisco, California, U.S.A., May 2004, post-deadline paper CPDD3, 2004.

32. M. Fuochi, J.R. Hayes, K Furusawa, W. Belardi, J.C. Baggett, T.M. Munro, and D.J. Richardson, Polarization mode dispersion reduction in spun large mode area silica holey fibers, Opt. Express, **12**, 1972–77 (2004).

33. J.L. Gimlet and N.K. Chaung, Effects of phase to intensity noise generated by multiple reflection on Gigabit per second DFB laser transmission systems, J. Lightwave Technol., **7**, 888 (1989).

34. C.J.S. de Matos, J.R. Taylor, T.P. Hansen, K.P. Hansen and J. Broeng, All-fiber chirped pulse amplification using highly dispersive air-core photonic bandgap fiber, Opt. Express, **11**, 2832 (2003).

35. H. Lim and F.W. Wise, Control of dispersion in a femtosecond ytterbium laser by use of hollow-core photonic bandgap fiber, Opt. Express, **12**, 2231 (2004).

36. W. Gobel, A. Nimmerjahn, and F. Helmchen, Distortion-free delivery of nanojoule femtosecond pulses from a Ti:sapphire laser through a hollow-core photonic crystal fiber, Opt. Lett., **29**, 1285 (2004).

37. G. Humbert, J.C. Knight, G. Bouwmans, P.St.J. Russell, D.P. Williams, P.J. Roberts and B.J. Mangan 2004, Hollow core photonic crystal fibers for beam delivery, Opt. Express, **12**, 1477 (2004).

38. B.J. Mangan, L. Farr, A. Langford, P.J. Roberts, D.P. Williams, F. Couny, M. Lawman, M. Mason, S. Coupland, R. Flea, and H. Sabert, Low loss (1.7 dB/km) hollow core photonic bandgap fiber, OFC 2004, postdeadline paper #24, 2004.

39. Y. Jiang, B. Howley, Z. Shi, Q. Zhou, R.T. Chen, M.Y. Chen, G. Brost, and C. Lee, Dispersion-enhanced photonic crystal fiber array for a true time-delay structured X-band phased array antenna, IEEE Photon. Technol. Lett., **17**, 187 (2005).